Electronic Supplementary Material (ESI) for Nanoscale.

Development and characterization of antibody reagents for detecting nanoparticles

Authors: Supriya Ravichandran[1], Mark A. Sullivan[2], Linda M. Callahan[3], Karen L. Bentley[3], Lisa A. DeLouise[1,4]

SUPPLEMENTARY FIGURES

[1]Department of Biomedical Engineering, University of Rochester, Rochester, New York 14642, USA.
[2]Department of Microbiology and Immunology, University of Rochester Medical Centre, Rochester, New York 14642, USA.
[3] Department of Pathology and Laboratory Medicine, University of Rochester Medical Centre, 601 Elmwood Avenue, Box 626, Rochester, New York 14642,
[4]Department of Dermatology, University of Rochester Medical Centre, Rochester, New York 14642, USA.
*email: Lisa_DeLouise@urmc.rochester.edu

Supplementary Table 1

a

Light Chain

CLONE	CDR1	CDR2	CDR3
GSH43	LPVLTQPPSASGSPGQRVTISCSGS **SSNIGSNTVN** WYQQLPGTAPKLLIY **SNNQRPS** GVPDRFSGSKSGTSASLAISGLRSEDEADYYCAA **WDDSLNG** WVFGGGTKLTVLG		
Ti49	SSELTQDPAVSVALGQTVRITC **QGDSLRSYYAS** WYQQKPGQAPVLVIY **GKNNRPS** GIPDRFSGSSSGNTASLTITGAQAEDEAEYYCYS **RDRSGNR** VIFGGGTKVTVLG		

b

Heavy Chain

CLONE	CDR1	CDR2	CDR3
GSH43	QVQLQQSGAEVKKPGASVKVSCKASGYTFN **THGFS** WVRQAPGQGLEWMGW **ISASNGNTKYPQNLQG** RVTMTVDTFTTTAYLELRSLRSDDTAVYYCVR **DRTDYYVPGTFDPLYGPFDY** WGQGTLVTVSS		
Ti49	QVQLESGPGLVKPSETLSLACTVSGGSIT **SSSYYWG** WIRQPPGKGLEWIG **SMSYRGTTYYNPSLES** RAIISADTAKNQFSLNLNSVTAADTAVYYCAR **WHCSSSMCYDLDY** WGPGTLVTVSS		

Supplementary Table 1: Amino acid sequences of **(a)** light and **(b)** heavy chain of GSH43 and Ti49 clones. The CDRs in each sequence are in bold typeface and underlined.

Supplementary Figure S1

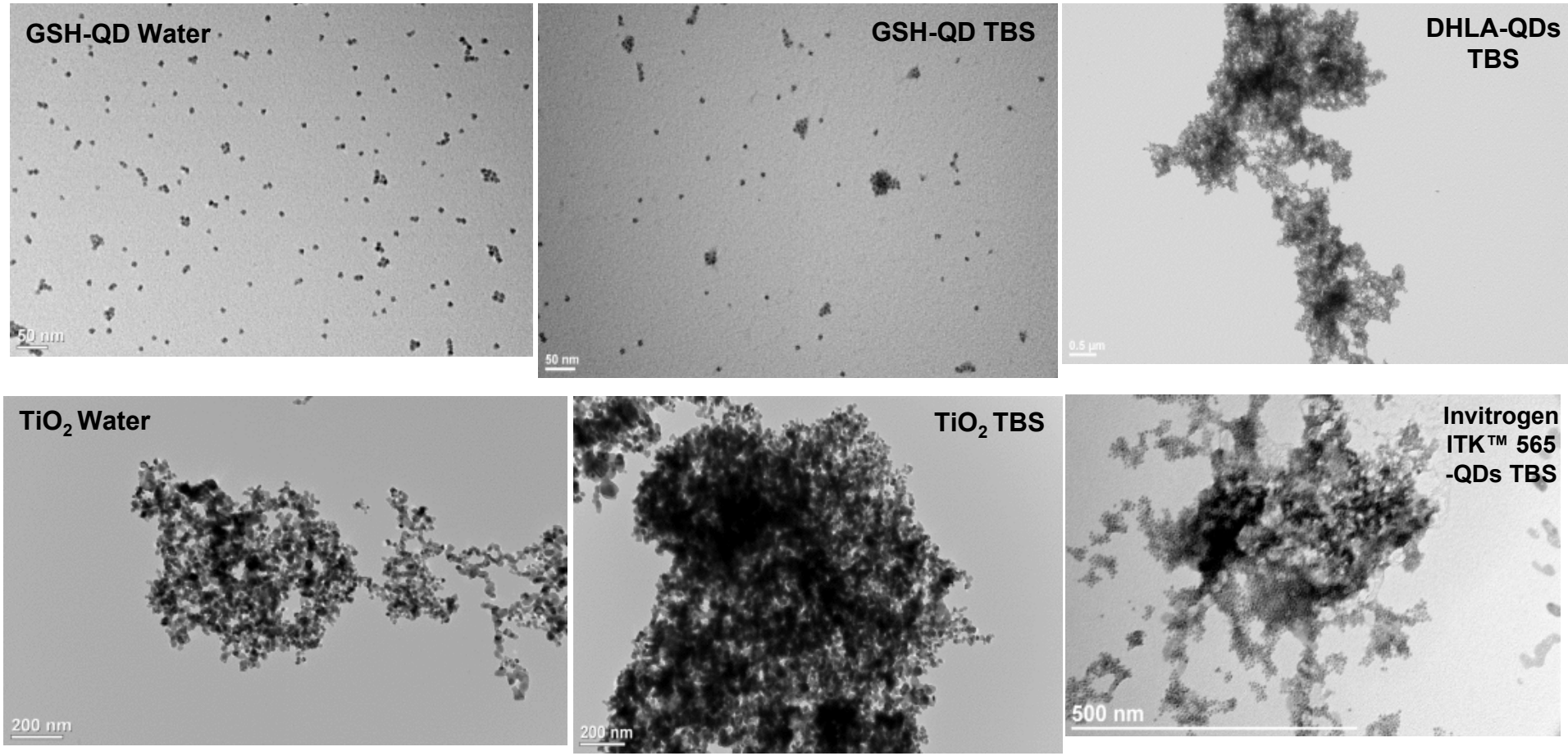

Supplementary Figure S1: TEM images of different NPs in water and TBS. GSH-QDs in water and TBS showing superior stability (Scale bar=50 nm) compared to TiO2 (Scale bar=200 nm) exhibiting agglomeration. DHLA-QDs and Invitrogen ITK™ 565-QDs in TBS showing agglomeration. Scale bar=500 nm.

Supplementary Figure S2

a

GSH-QD

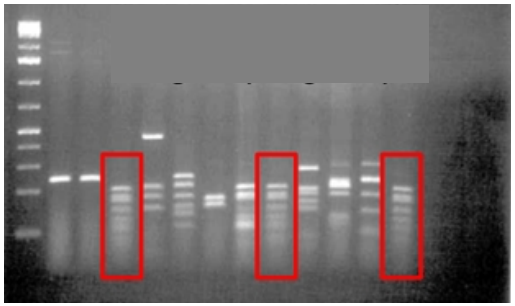

b

TiO_2 NP

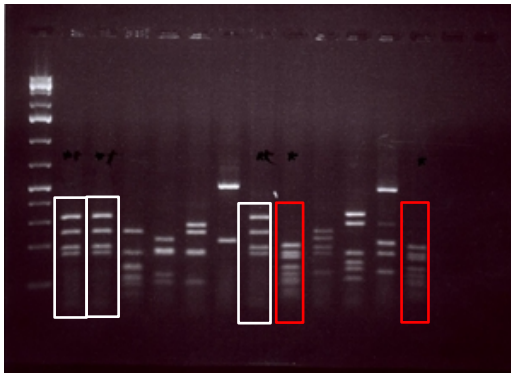

Supplementary Figure S2: Pattern repeats of scFvs (**red** and **white** boxes) generated by panning on (a) GSH-QDs and (b) TiO_2 NPs following a BstNI digest after Round 4 of panning.

Supplementary Figure S3

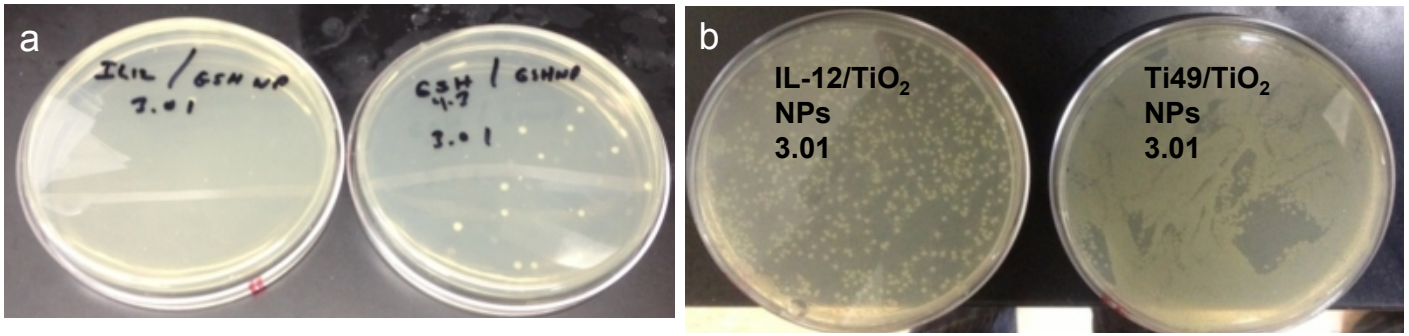

Supplementary Figure S3: **Image of titer plates.** Centrifugation phage titer indicating high binding of phage clone to respective NP target relative to off-target negative control IL-12 phage clone. Plate label indicates Phage clone/NP type and the number indicates phage dilution factor. 3.01 dilution factor indicate 1:1000 of phage diluted in TBS and 10µl was used to infect bacteria cells. **(a)** Phage titer colonies showing ~10-fold more enrichment of GSH43ϕ on GSH-QDs compared to negative control IL-12ϕ on GSH-QDs. **(b)** Phage titer colonies showing ~100-fold more enrichment of Ti49ϕ on TiO2 NP compared to IL-12ϕ on TiO_2 NPs.

Supplementary Figure S4

GSH43ϕ binding GSH-QDs

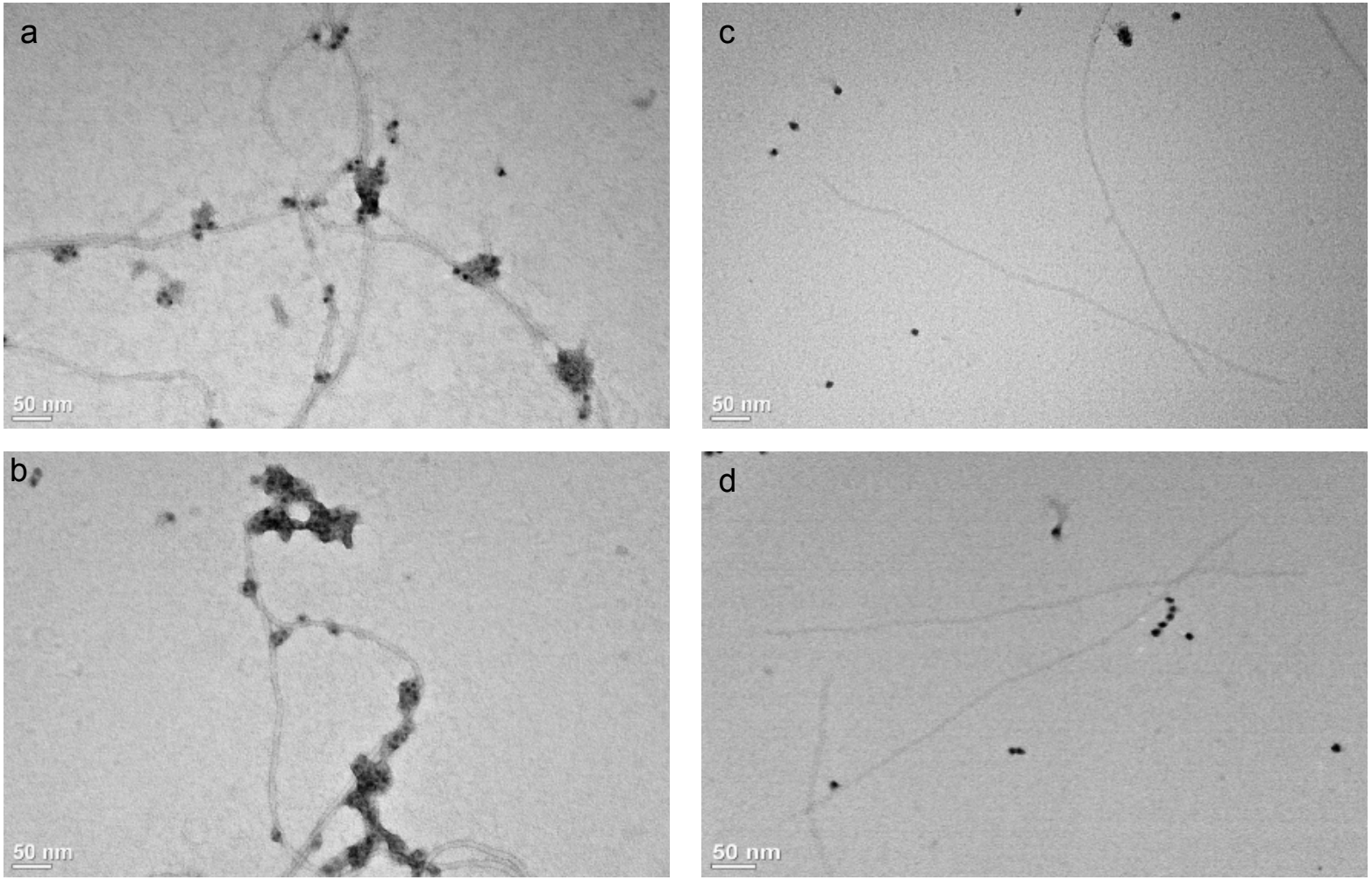

IL12ϕ not binding GSH-QDs

Supplementary Figure S4: Other TEM images of GSH43ϕ and IL12ϕ each mixed separately with GSH-QDs. **(a,b)** GSH43ϕ exhibit strong association and clustering with GSH-QDs whereas **(c,d)** the negative control IL-12ϕ shows no affinity for the GSH-QDs which appear highly dispersed. Scale bar=50 nm.

Supplementary Figure S5

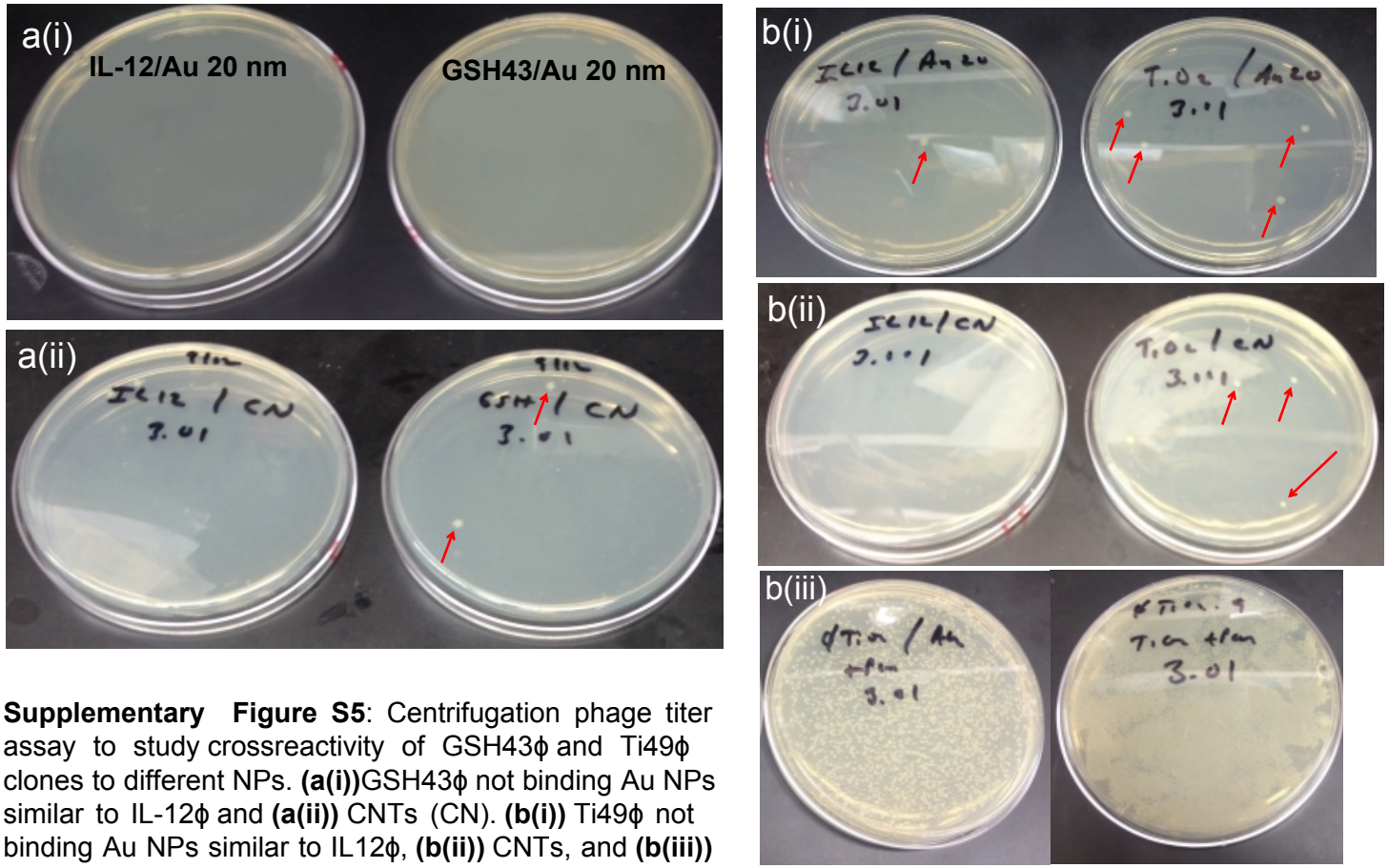

Supplementary Figure S5: Centrifugation phage titer assay to study crossreactivity of GSH43ϕ and Ti49ϕ clones to different NPs. **(a(i))**GSH43ϕ not binding Au NPs similar to IL-12ϕ and **(a(ii))** CNTs (CN). **(b(i))** Ti49ϕ not binding Au NPs similar to IL12ϕ, **(b(ii))** CNTs, and **(b(iii))** Au powder (left) compared to TiO_2 NPs (right) which is more than 100-fold. **Red arrows** indicate colonies not visible clearly. All phage titers were performed at the same dilution (3.01 indicating, 1:1000 phage diluted in TBS and 10 µL used to infect bacterial host cells).

Supplementary Figure S6

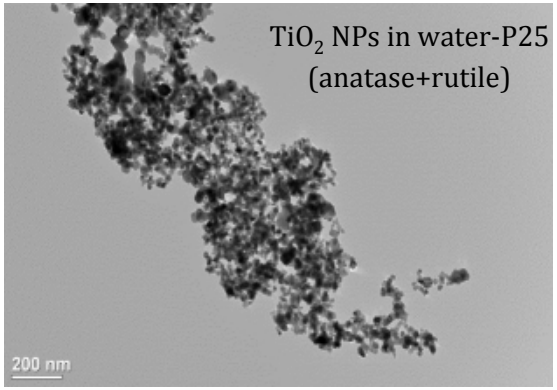

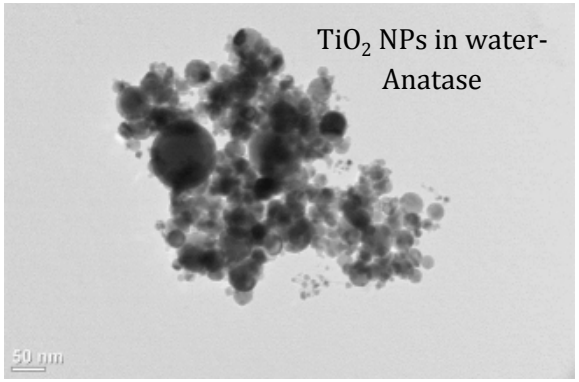

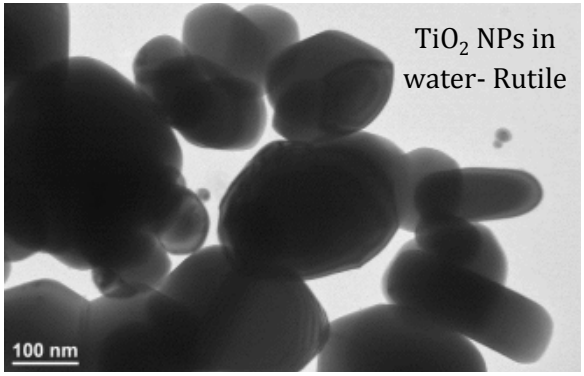

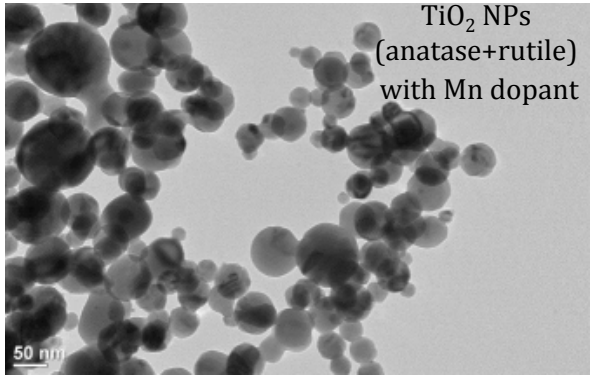

Supplementary Figure S6: TEM Images of TiO_2 NPs. TEM images showing morphology and sizes of various TiO_2 NPs including anatase+rutile (P25), anatase only, rutile only and TiO_2 NPs with 1% Mn as dopant in water. Scale bar= 200, 50, 100, 50 nm respectively.

Supplementary Figure S7

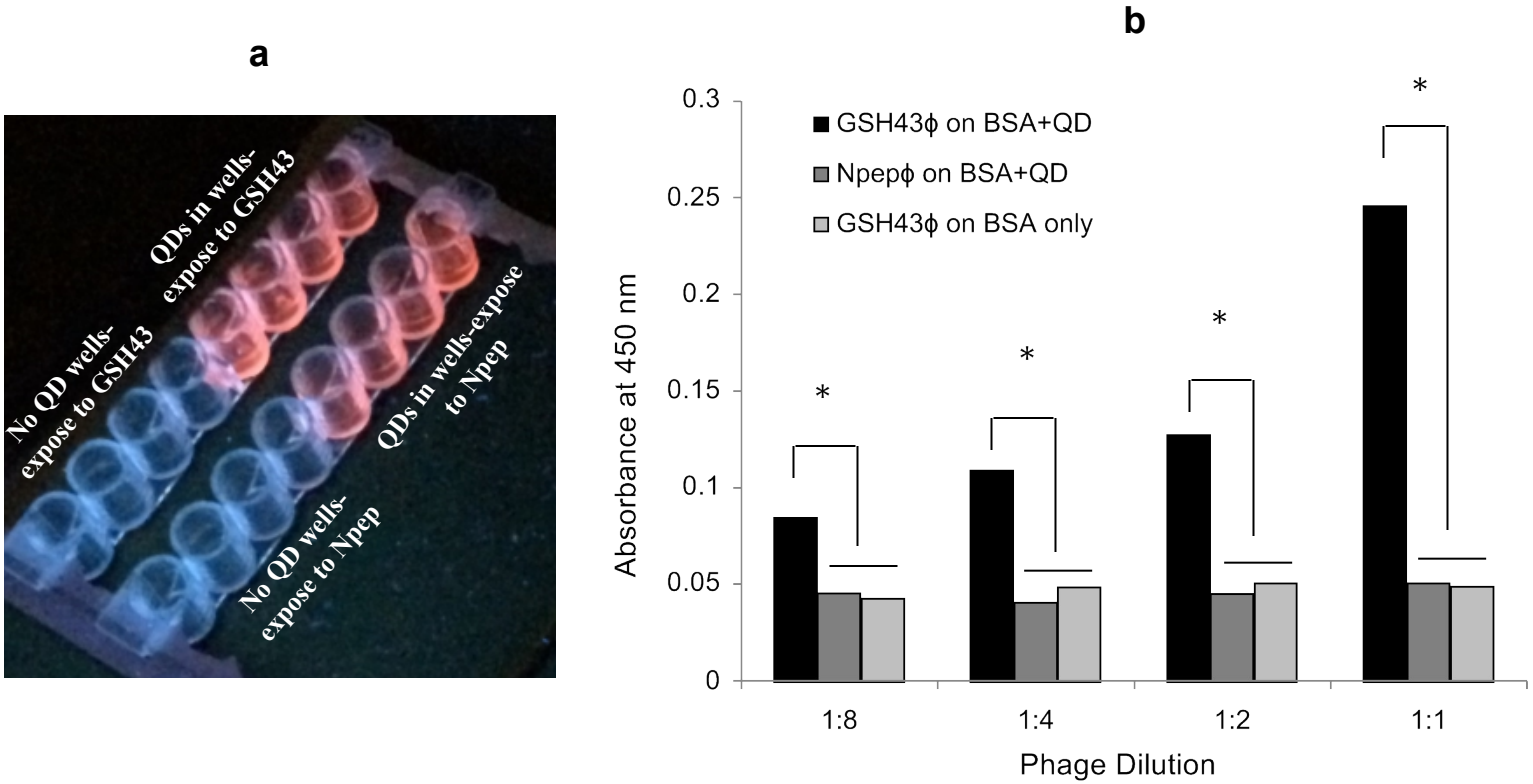

Supplementary Figure S7: **(a)** QDs immobilized on a BSA-coated plated as visible under a UV-lamp whereas wells with no QDs do not fluoresce. **(b)** Phage ELISA assay of GSH43ϕ and negative control (Npepϕ) on QDs immobilized on BSA-coated plates. With an increasing concentration of phage, significantly more binding (*$p<0.05$) of GSH43ϕ to GSH-QDs occurs when detected using TMB substrate at 450 nm, compared to negative control Npepϕ and GSH43ϕ interacting with wells containing BSA alone (no QDs). Values are average of three independent experiments and error bars represent SEM. Statistics was performed using two-tailed unpaired student's t-test.

Supplementary Figure S8

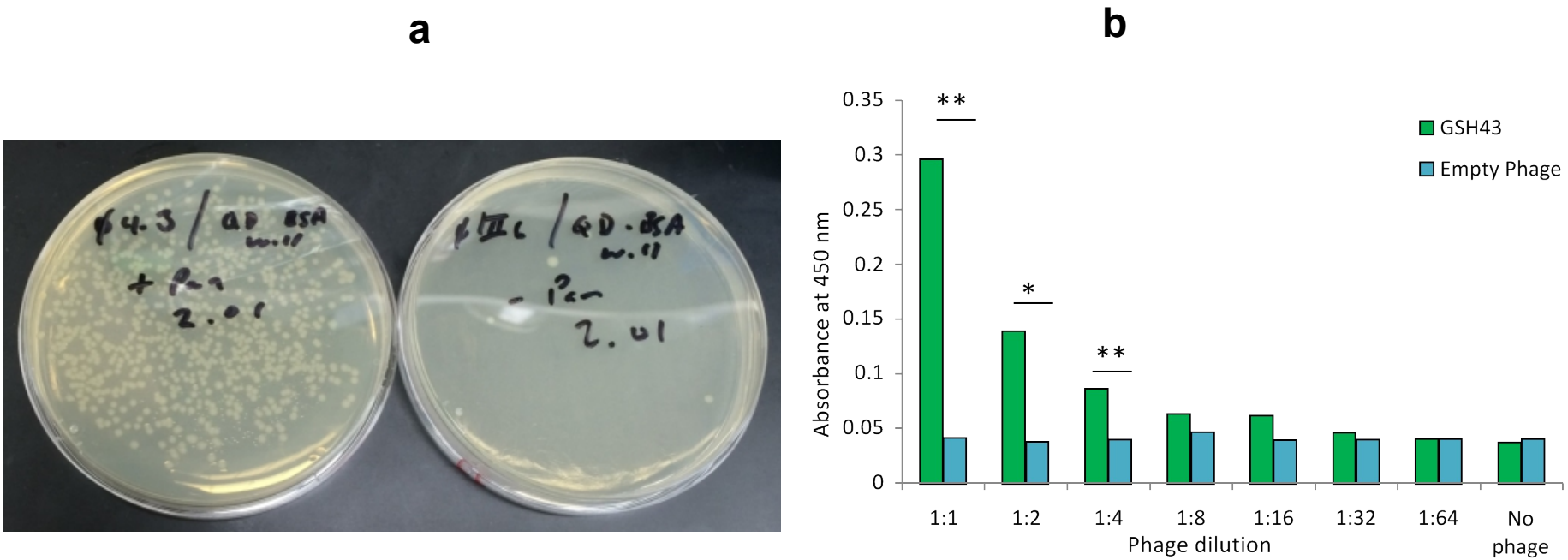

Figure S8: Comparison of GSH43ϕ to empty vector ϕ in binding to GSH-QDs. (a) : Titer images comparing empty vector phage and GSH43ϕ binding GSH-QDs. Plate titer images showing GSH43ϕ (left) exhibiting binding to GSH-QDs (~200-fold) immobilized on BSA, whereas negative control empty phage (not displaying an antibody, right) does not. Labels are of the format phage/target NP and the number indicates dilution. 2.01 represents 1:100 dilution of phage and 10 µL of phage was used to infect TG1 cells **(b)** Plot showing binding of GSH43ϕ relative to empty vector to GSH-coated wells in a phage ELISA assay. GSH43ϕ binds GSH (green bars) significantly over background binding exhibited by negative control empty phage (blue bars). A student's unpaired t-test was used to determine significance, **p<0.01, *p=0.01. Data plotted are average of two independent experiments and error bars represent SEM.

Supplementary Figure S9

a

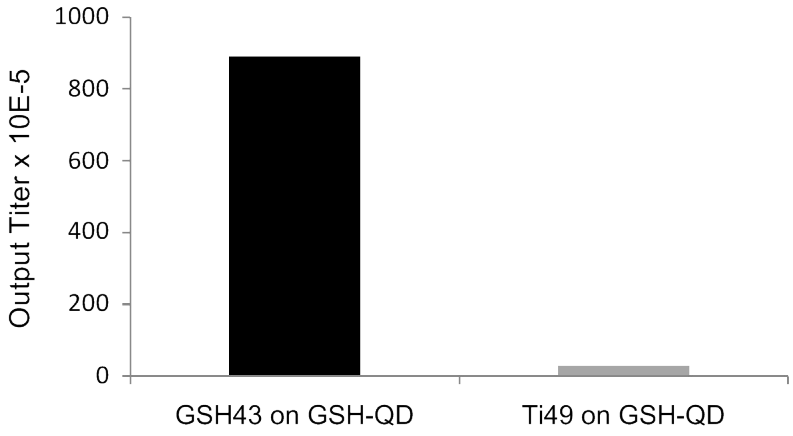

b

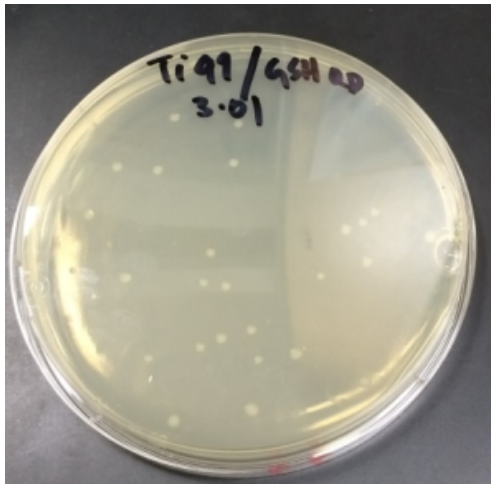

Supplementary Figure S9: Absence of crossreactivity of Ti49 clone to GSH-QDs. (a) Plot showing output titers of GSH43ϕ and Ti49ϕ on GSH-QDs where there is no binding of Ti49ϕ clone to GSH-QDs (~30) compared to GSH43ϕ clone (~900) upon a panning assay where GSH-QDs were immobilized on a BSA coated plate. (b) Image of the plate showing ~30 colonies upon titering the Ti49ϕ on GSH-QDs sample.

Supplementary Figure S10

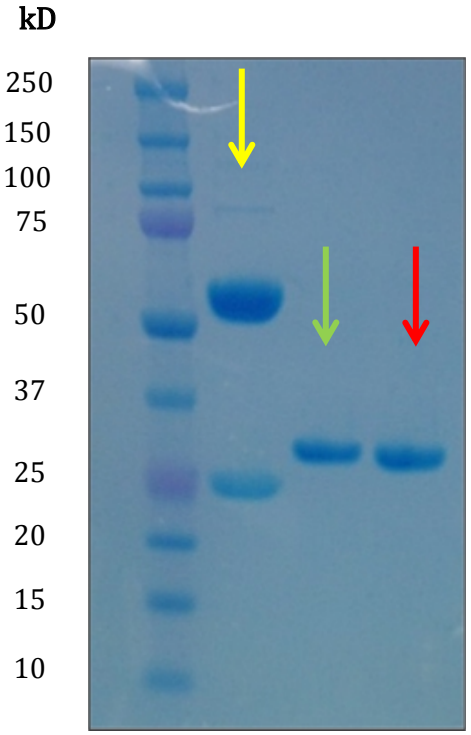

Figure S10: Representative SDS-PAGE Gel. Figure shows presence of purified GSH43-scFv (green arrow) and negative control (NT3-scFv, red arrow)-scFvs indicated by the blue bands (25 kD) compared to a whole antibody control (YerVoy antibody, yellow arrow).

Supplementary Figure S11

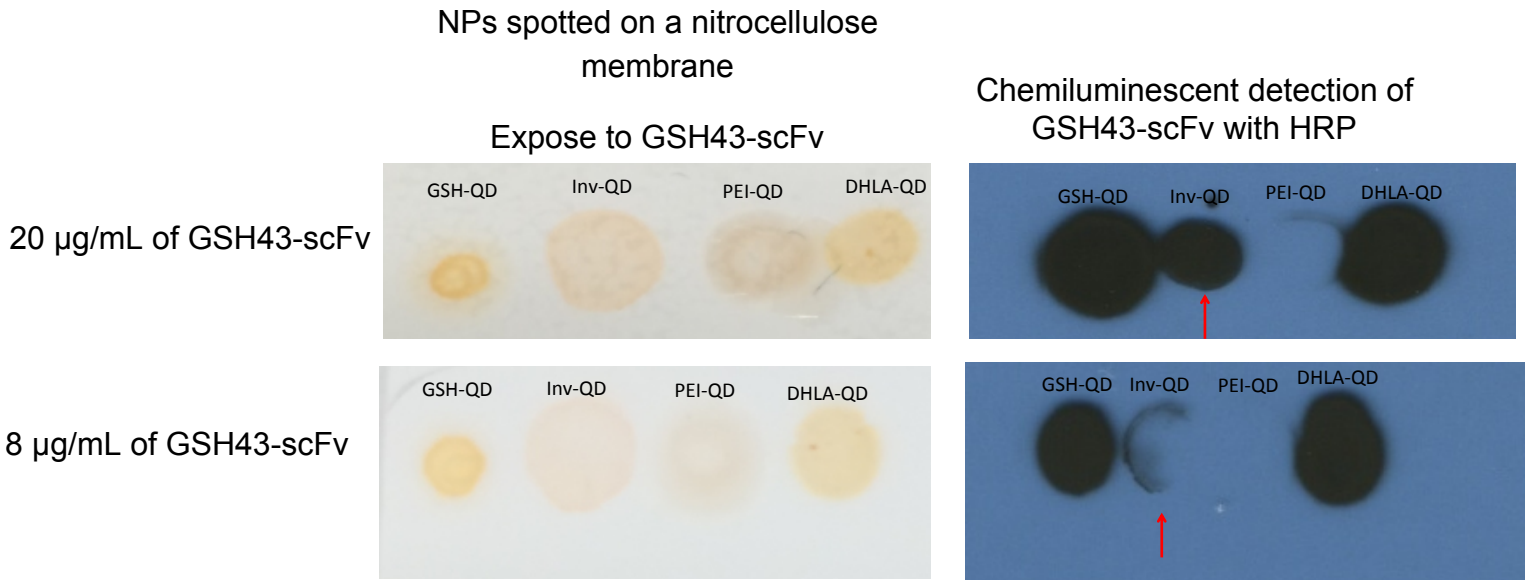

Supplementary Figure S11: Dot blot to verify binding of GSH43-scFvs at different concentrations to Invitrogen ITK™ 565-QDs (Inv-QDs, 1 µL) spotted on a nitrocellulose membrane. GSH43-scFv binds Invitrogen QDs at 20 µg/mL and 8 µg/mL but not 5 µg/mL as discussed in Figure 2. Red arrows detect spot formed upon chemiluminescent detection using HRP indicative of binding to Inv-QDs.

Supplementary Figure S12

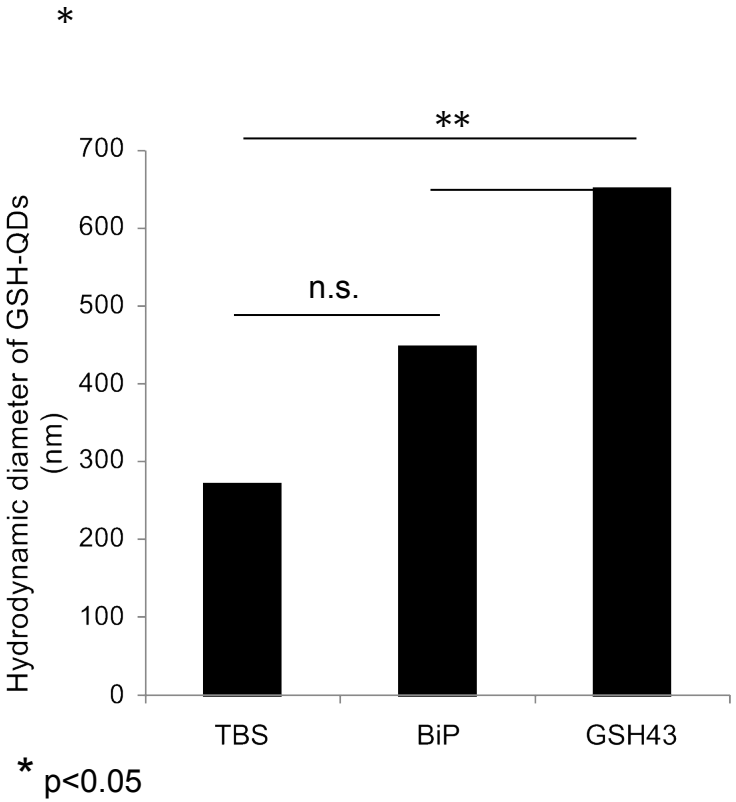

Supplementary Figure S12: Hydrodynamic diameter measurements using the Malvern Zetasizer on GSH-QD mixed 2 hr with BiP or GSH43 scFvs, centrifuged, and resuspended in TBS:water (3:7). GSH43-scfv-QD conjugate shows a significant increase in hydrodynamic diameter compared to BiP-associated QDs ($p<0.05$) and QDs processed in TBS alone ($p<0.01$) using a one-way ANOVA test, whereas BiP-associated complexes do not show any significance (n.s.) compared to QDs in TBS. Error bars indicate SEM of 4 independent experiments.

Supplementary Figure S13

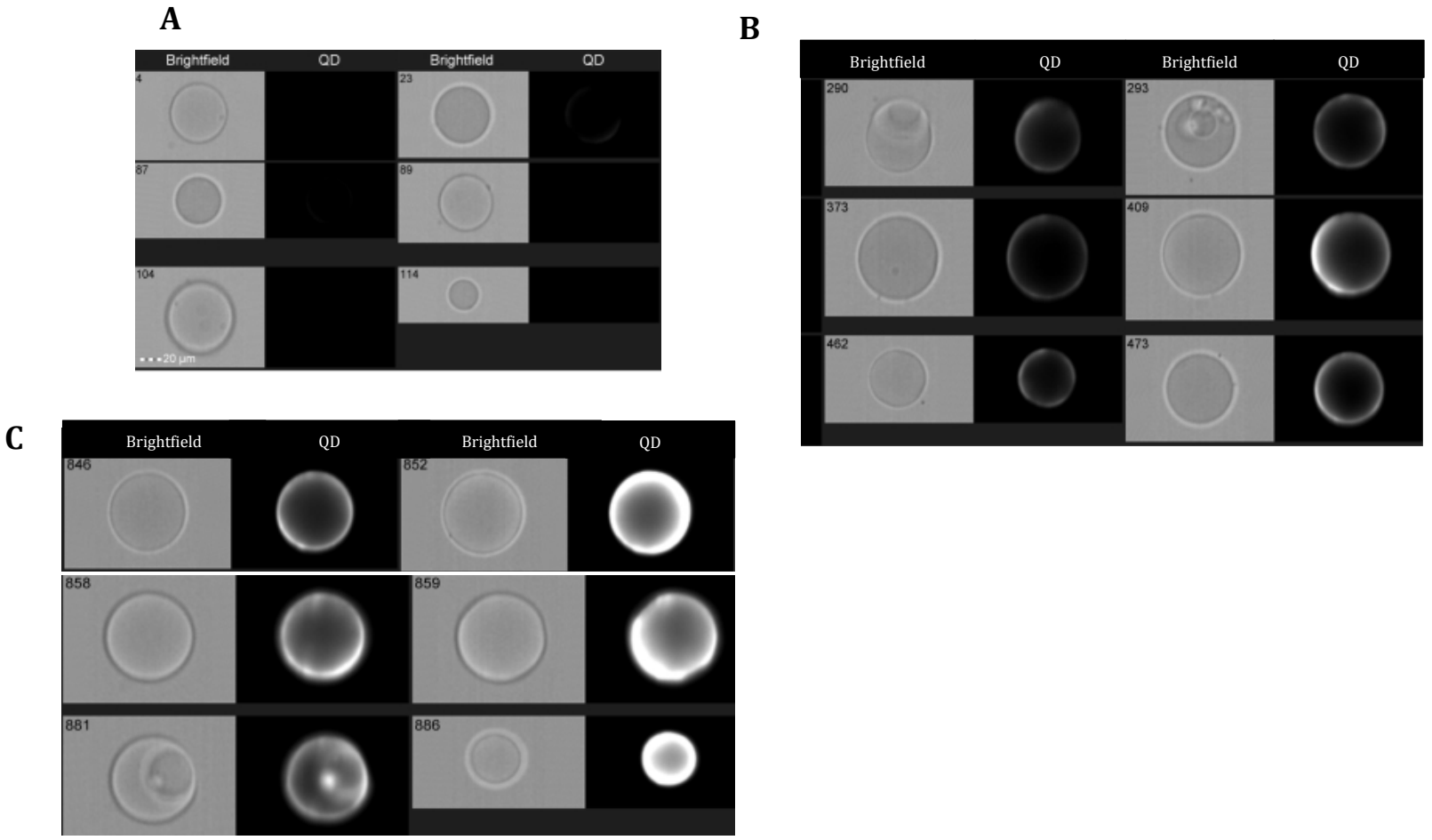

Figure S13: Image Stream Experiment Using Beads. Representative images showing brightfield and QD channels of anti-FLAG coated agarose beads flowing through Image Stream flow cytometer where A) represents beads not coated with scFvs but treated with GSH-QDs. No QD fluorescence is seen in the images indicating that QDs did not nonspecifically bind anti-FLAG coated agarose beads. However, upon coating beads with B) negative control BiP-scFv shows a weak background QD signal is detected however, coating beads with C) GSH43-scFv show intense QD fluorescence exposure indicating the binding of the GSH-QDs to GSH43-scFvs. Scale bar=20 µm.

Supplementary Figure S14

a

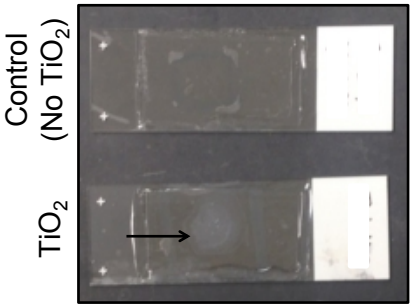

b

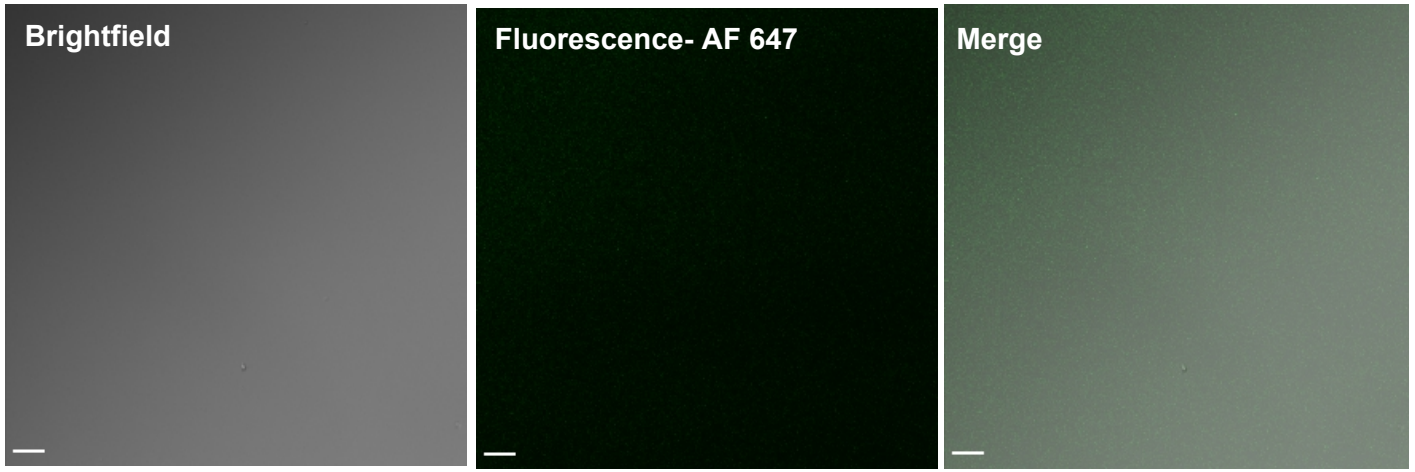

Supplementary Figure S14: **(a)** Slides showing TiO_2 in water dried indicated by the black arrow (**bottom**) whereas control shows no white spot (**top**). **(b)** Confocal images of slide without TiO_2 NPs incubated with Ti49-scFvs followed by detection with Alexa Fluor 647-(pseudo-color **green**) conjugated anti-FLAG antibody. No non-specific staining was observed. Scale bar=20 μm.

Supplementary Figure S15

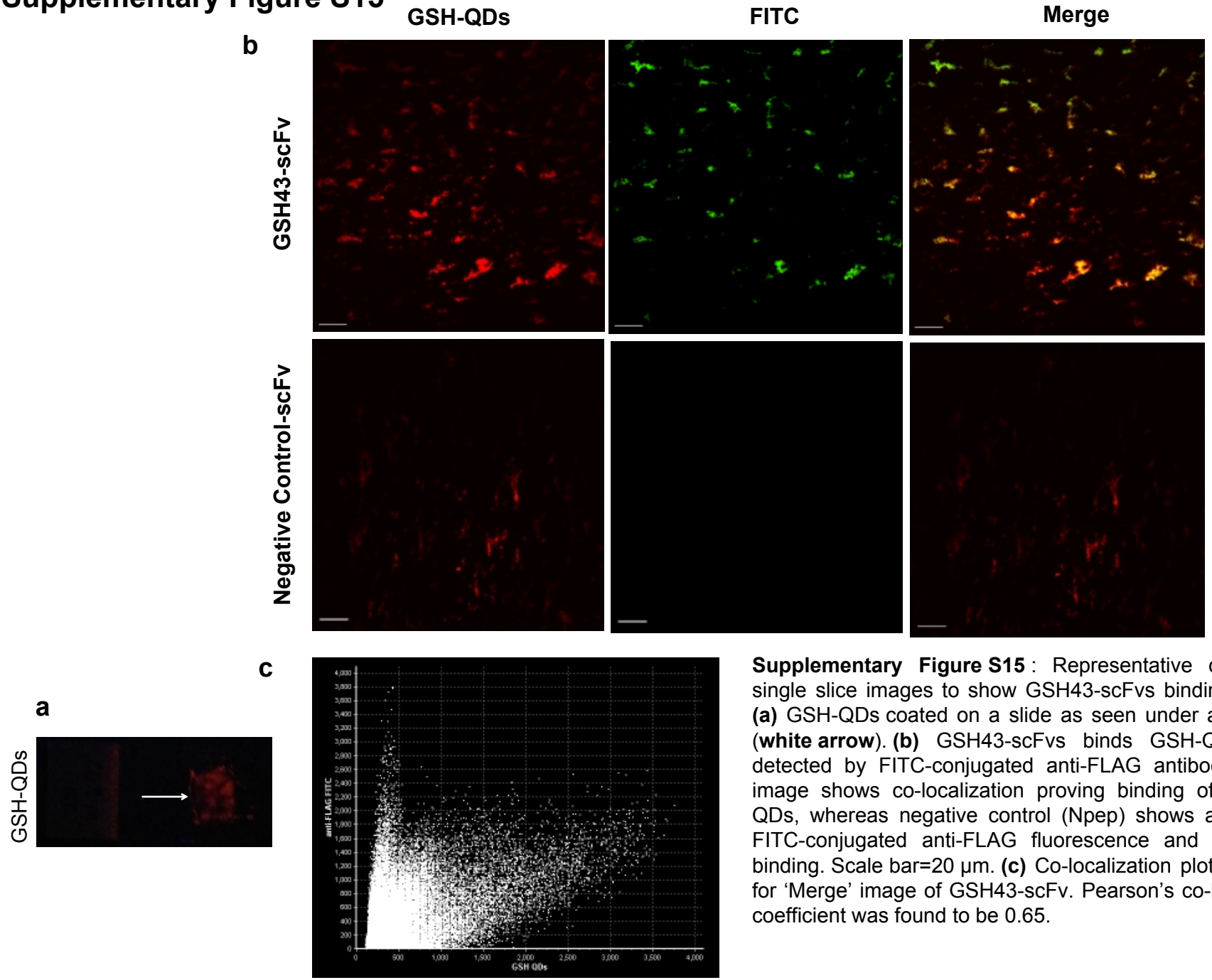

Supplementary Figure S15 : Representative confocal single slice images to show GSH43-scFvs binding to QDs. **(a)** GSH-QDs coated on a slide as seen under a UV lamp (**white arrow**). **(b)** GSH43-scFvs binds GSH-QDs as detected by FITC-conjugated anti-FLAG antibody. Merge image shows co-localization proving binding of scFvs to QDs, whereas negative control (Npep) shows absence of FITC-conjugated anti-FLAG fluorescence and hence no binding. Scale bar=20 µm. **(c)** Co-localization plot obtained for 'Merge' image of GSH43-scFv. Pearson's co-localization coefficient was found to be 0.65.

Supplementary Figure S16

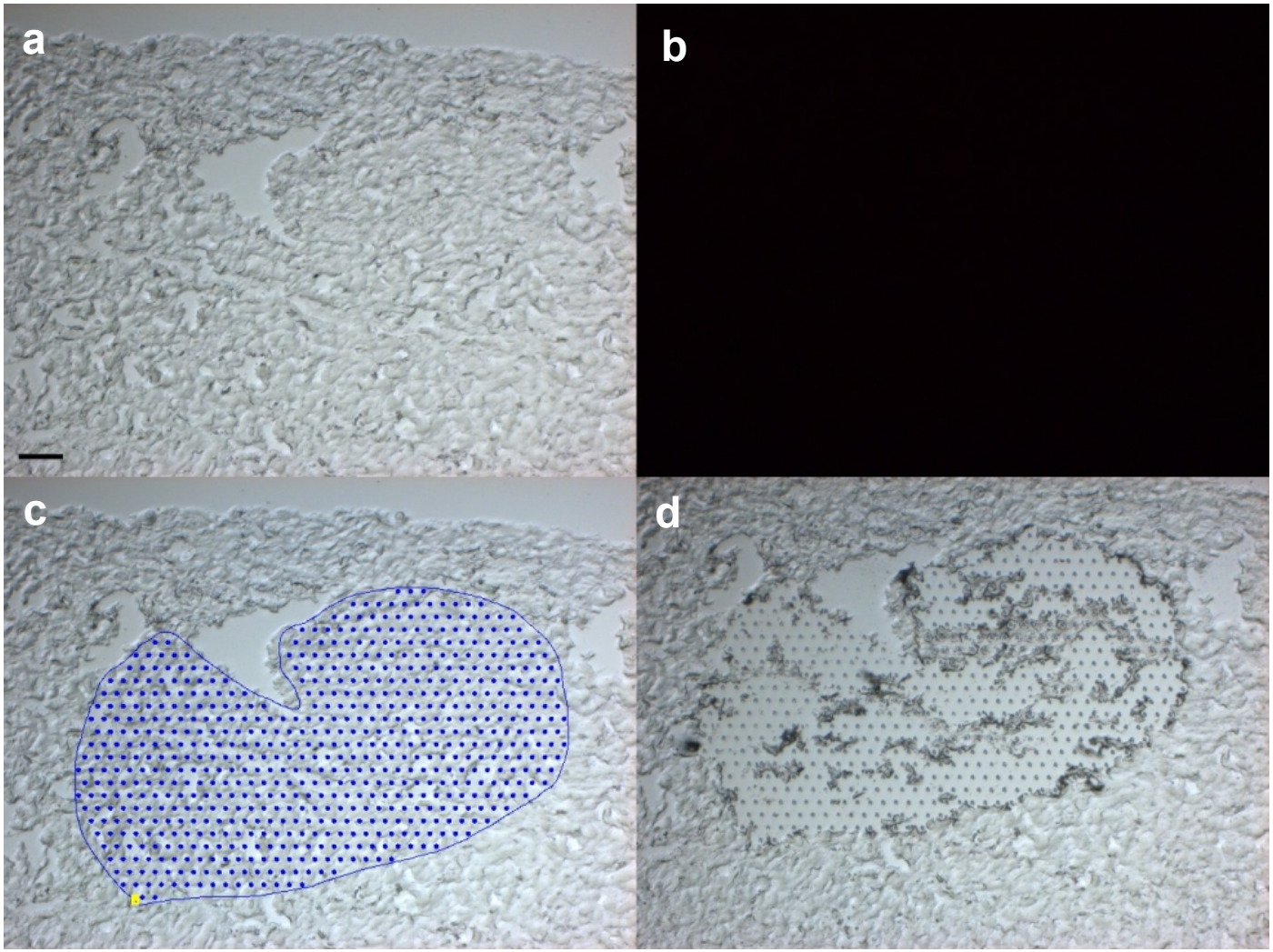

Supplementary Figure S16: LCM imaging of control 'no QD' sample of *ex vivo* human skin. Representative control sample showing **(a)** no AP staining indicating lack of binding of GSH43-scFvs to GSH-QDs. **(b)** Complete absence of GSH-QDs (no fluorescence). **(c)** Portions of tissue sections were marked for cut and captured onto adhesive tube caps using LCM, and processed for AAS. **(d)** The portion of skin remaining after capture is shown. Scale bar=50 µm.

Supplementary Figure S17a

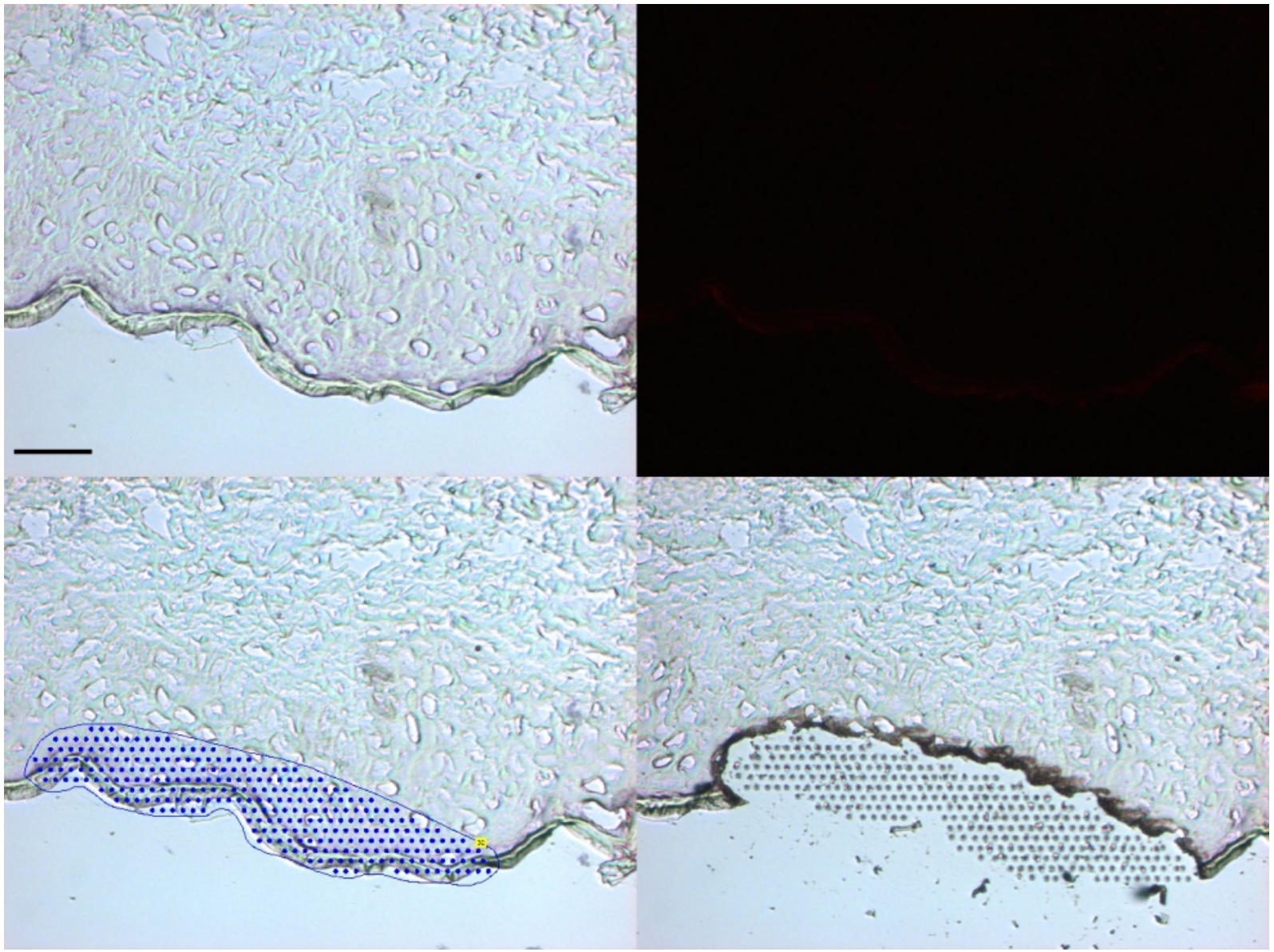

Supplementary Figure S17b

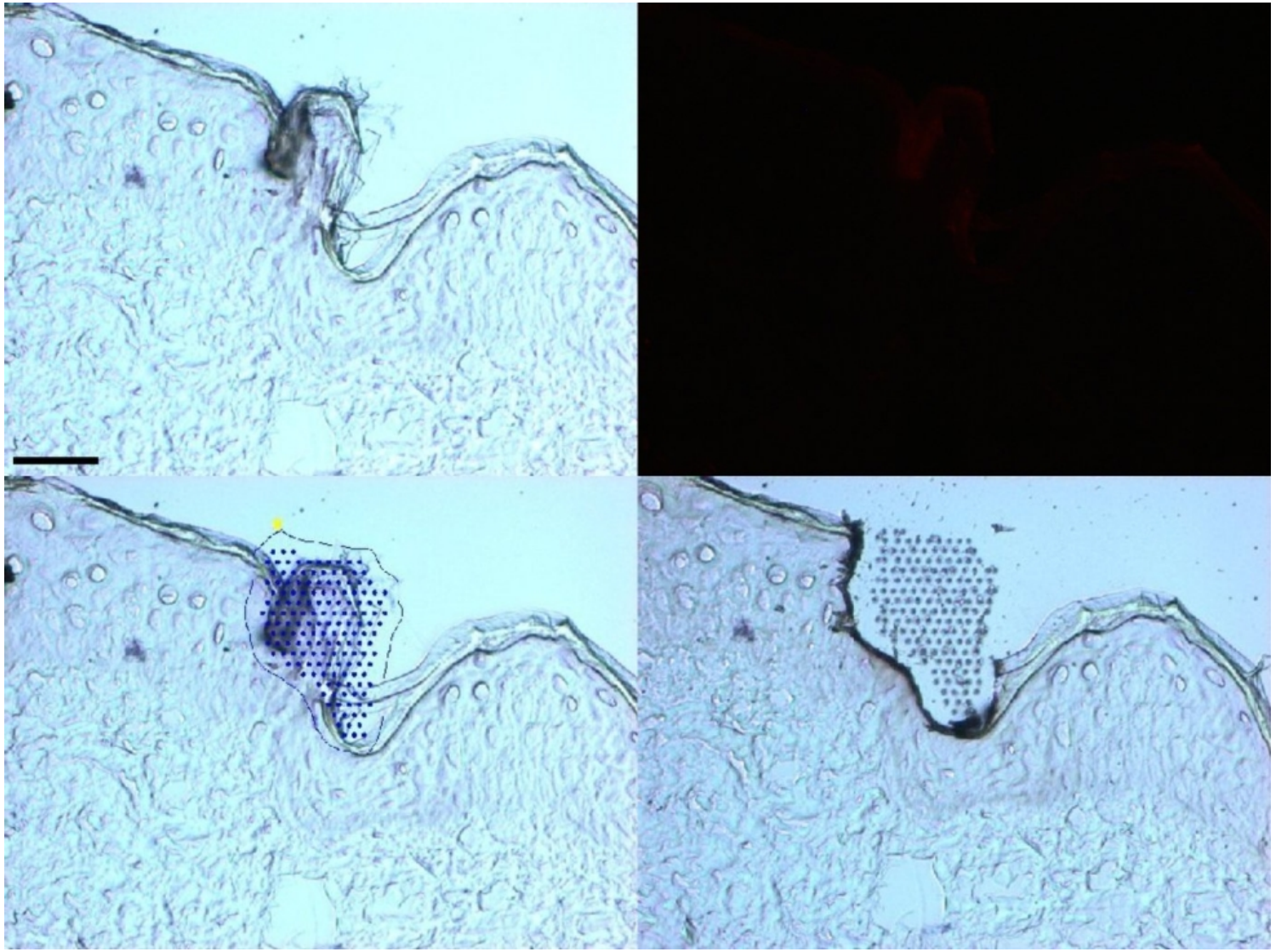

Supplementary Figure S17c

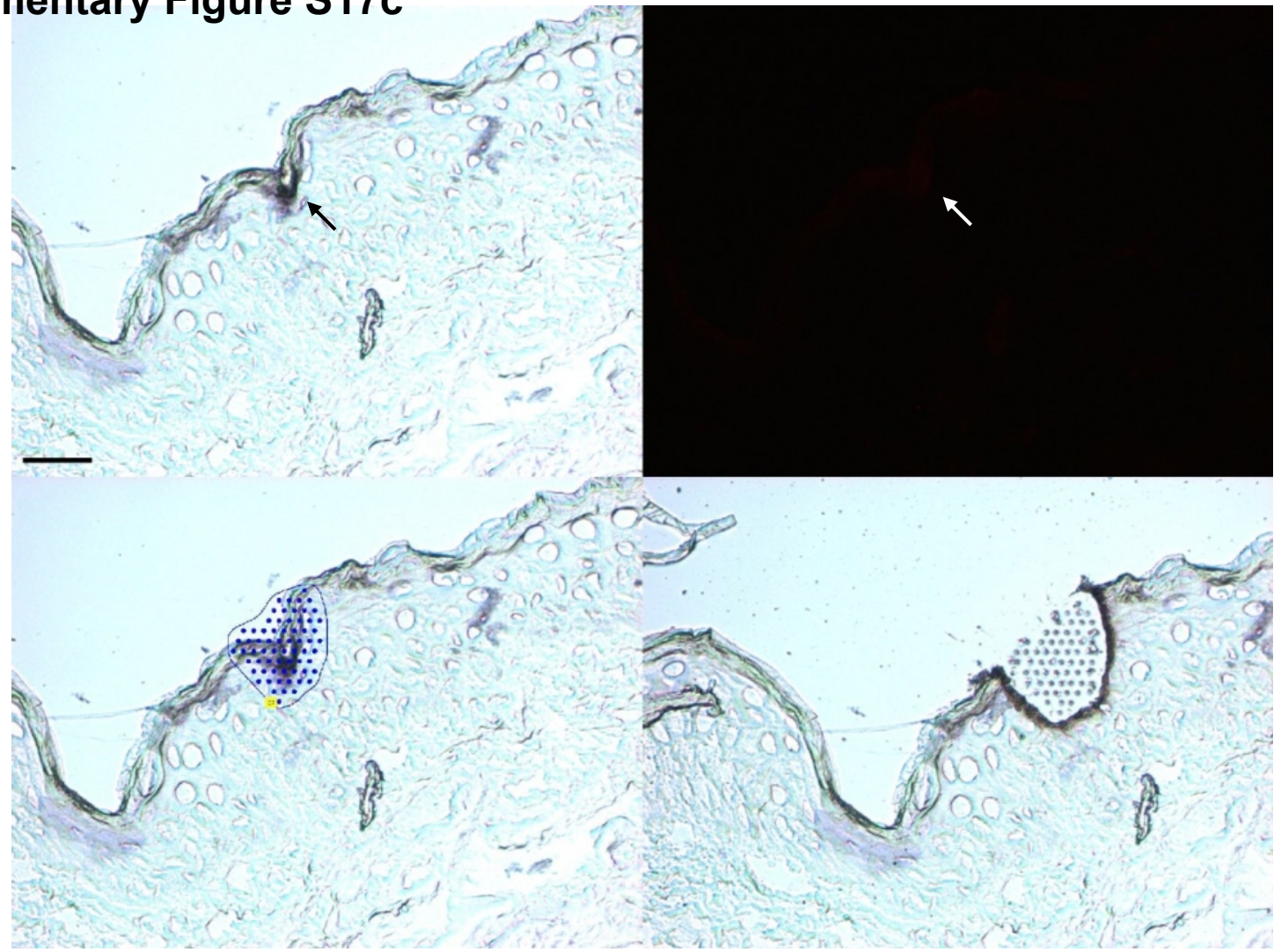

Supplementary Figure S17: Representative images to prove binding of GSH43-scFvs to GSH-QDs applied on epidermis using LCM and AAS. **(a)** Control skin specimen not treated with QDs showing no AP staining in brightfield (**top-left**) and no fluorescence (**top-right**). Upon using LCM to cut and capture (**bottom-left, bottom-right**) portions of skin for AAS analysis, Cd levels (0.0085 ng/mL) were found to be <LOQ (0.025 ng/mL). **(b)** GSH-QDs applied on epidermis shows binding to GSH43-scFvs detected by AP (**top-left**). A portion with visible staining and fluorescence (**top-right**) was marked for cut (**bottom-left**) and captured (**bottom-right**) for AAS analysis. Cd levels were found to be 0.108 ng/mL proving presence of QDs. **(c)** Areas where AP staining was visible (**top-left**) but not fluorescence (**white arrow**, **top-right**), however when samples was marked for cut (**bottom-left)** and captured (**bottom-right**) using LCM, and analyzed using AAS, Cd levels were found to be 0.018 ng/mL which was greater than control. Scale bar=50 µm.

Supplementary Figure S18

a

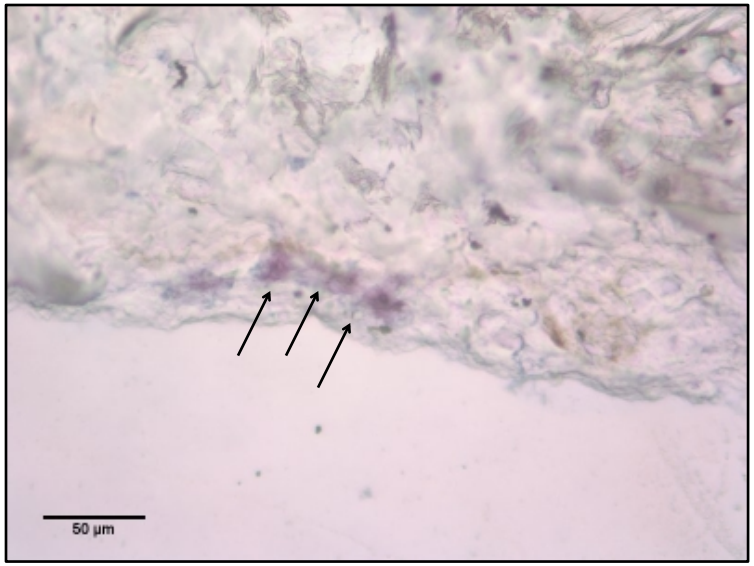

b

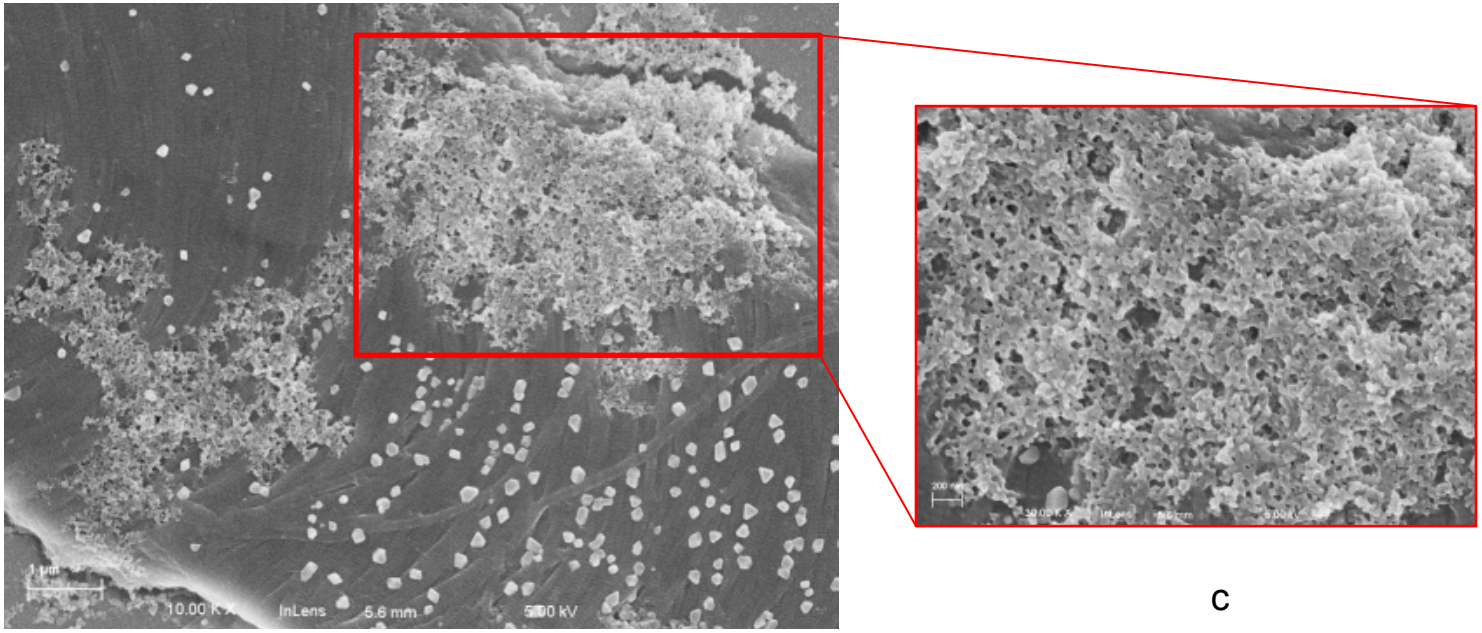

c

Supplementary Figure S18: Positive control human *ex vivo* skin treated with TiO_2 NPs in the dermis of skin. IHC was performed with Ti49-scFvs to prove presence of TiO_2 NPs. (a) Bright-field image showing AP staining (black arrows) with the use of Ti49-scFvs in an *ex vivo* human skin sample upon application of 1 mg/mL TiO_2 NPs in the dermis. (b) SEM image showing TiO_2 NPs and (c) magnified image of the TiO_2 NPs in skin hence proving presence of NPs in the corresponding stained areas.

Supplementary Figure S19

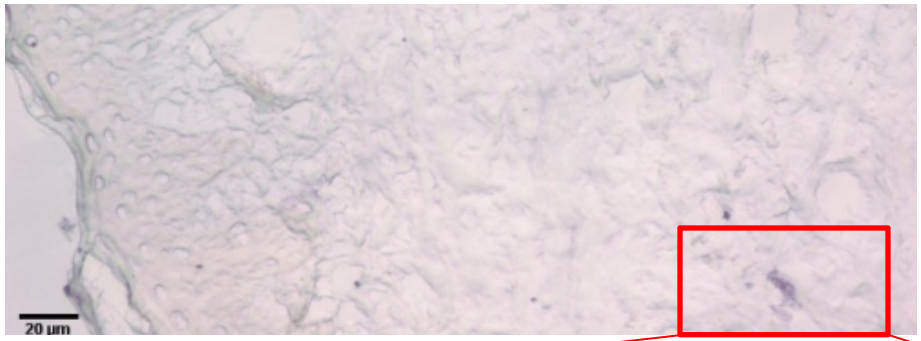

a

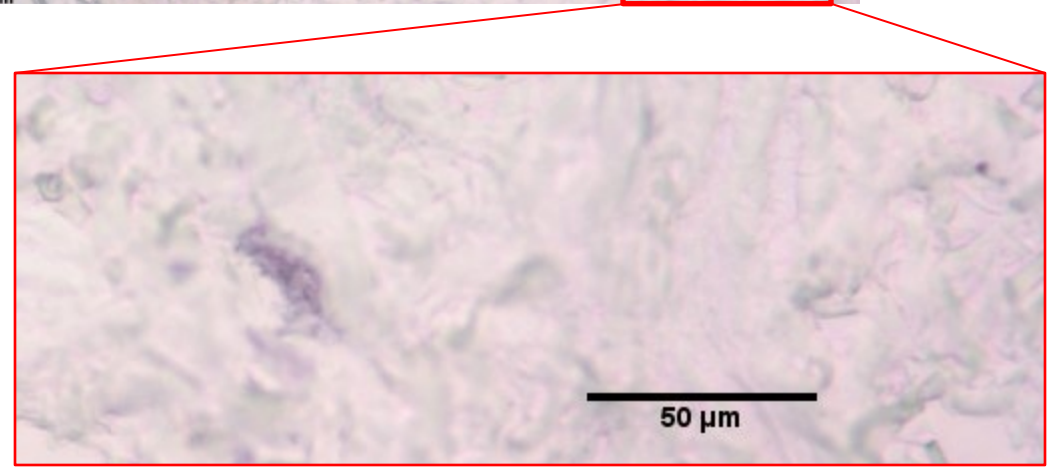

b

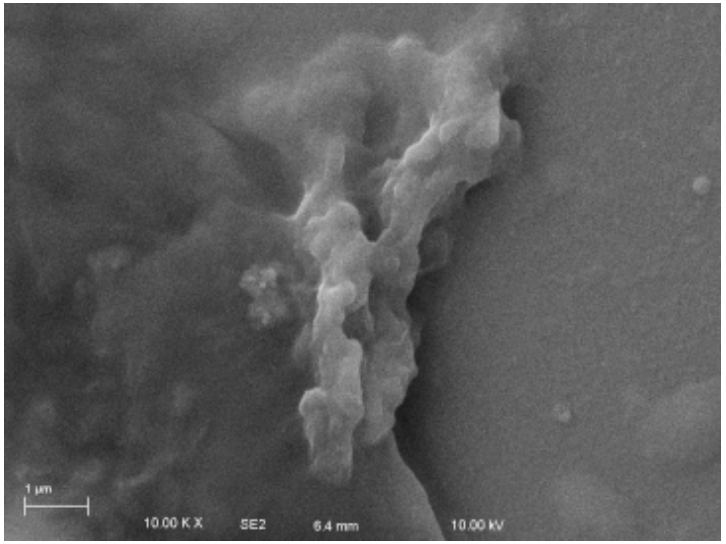

c

Supplementary Figure S19: Tape stripped ex vivo human skin sample treated with TiO_2 NPs showing (a) presence of AP staining in the dermis upon performing IHC with Ti49-scFvs. (b) Examination of the stained area using (c) SEM shows presence of TiO_2 NPs similar in morphology to the TiO2 in the epidermis, Supplementary Figure S17.